Journal of Applied Sciences 11 (7): 1411-1415, 2011
ISSN 1812-5654 / DOI: 10.3923/jas.2011.1411.1415

Effect of Calcination Process on Phase Formation in Nano-sized $Zn_{0.9}Mn_{0.1}O$ Particles

Majid Ebrahimizadeh Abrishami, Seyed Mohammad Hosseini and Ahmad Kompany
Materials and Electroceramics Laboratory, Department of Physics,
Ferdowsi University of Mashhad, Mashhad, Iran

Abstract: This study reports the effect of the calcination processes on the structural and mid-infrared optical properties of $Zn_{0.9}$ $Mn_{0.1}O$ nanopowders synthesized by sol-gel technique. X-ray diffraction analysis revealed that the synthesized nanopowders calcinated at low temperatures have mono-phase wurtzite structure. TEM images show that the average particle size is about 35 nm. By changing the calcination temperature, it was possible to decrease the percentage or even eliminate the presence of the secondary phases in the composition. The characterization was completed by studying the mid-infrared transmittance spectra using Fourier Transformation Infrared (FTIR) spectroscopy.

Key words: ZnO:Mn, nanopowder, sol-gel, secondary phase

INTRODUCTION

Zinc oxide is a wide band gap (3.34 eV) semiconductor stably crystallized in hexagonal (wurtzite) structure with space group P63mc and the lattice constants a = 3.25Å and c = 5.21 Å (Kisi and Elcombe, 1989). Because of its remarkable electrical and optical properties, ZnO has attracted much more attention to be used in thermoelectric (Ohtaki *et al*., 2009) and optoelectronic devices (Fonoberov and Balandin, 2006). Moreover, ZnO doped with the transition metals such as Mn, Co, Fe and Ni is a good candidate for fabricating Diluted Magnetic Semiconductors (DMS), as the new generation of electronic devices. In recent years, atom-like behavior of nanostructures has persuaded the researchers to synthesize the nanopowders of materials. Several wet chemical methods have been suggested to prepare ZnO:Mn nanopowders such as: gel-combustion (Noori *et al*., 2008), sol-gel (Xu *et al*., 2009) and co-precipitation (Yadav *et al*., 2009). In preparing nano-scale ZnO:Mn particles, it is very important to obtain mono-phase structure. In order to achieve this goal, one should consider three important facts: lowering the calcination temperature, increasing Mn solubility and control the growth of the second phases.

In this study, we used the sol-gel method to synthesize $Zn_{0.9}Mn_{0.1}O$ nanopowders. The effect of the calcination temperature on the phase formation and the lattice constants were investigated. FTIR was employed to perform a subtle analysis on the secondary phases and compare the results with the structural properties.

MATERIALS AND METHODS

The precursors for the synthesis of $Zn_{0.9}Mn_{0.1}O$ nanoparticles were zinc acetate dehydrate, $Zn(CH_3COO)_2.2H_2O$ (Merck), manganese acetate tetrahydrate, $Mn(CH_3COO)_2.4H_2O$ (Merck), acetic acid (Merck) and diethanolamine (DEA) (Merck). Appropriate amounts of zinc and manganese acetates were dissolved in a mixture of isopropanol and distilled water, stirring and heating at 40°C for 30 min. Then, a mixture of acetic acid and DEA was added to the cations solution. The whole solution was constantly stirred until it became clear with no precipitates. The molar ratio of acetic acid and DEA to cations was kept two and one, respectively. In order to obtain a clear sol, the whole solution with pH = 7 was refluxed for 4 h at 110°C. For preparing the gel, an 80°C heat bath was used to evaporate the solvents. Then, the obtained gel was dried at temperatures of 140-150°C. Finally, the resultant black powders were calcinated at 400, 500, 600, 700 and 800°C in air. The heating rate was chosen 3°C min^{-1} up to the calcination temperature, keeping the powders at this temperature for 2 h and then cooling down to room temperature with the rate of 2°C min^{-1}.

We studied the structural properties and optical characterizations of the samples using X-ray Diffraction

Corresponding Author: Ahmad Kompany, Materials and Electroceramics Laboratory, Department of Physics, Ferdowsi University of Mashhad, Mashhad, Iran

(XRD; model: Siemens D500) analysis, Transmission Electron Microscopy (TEM; LEO 912AB-Germany) and transmittance spectra (in the range of 400-2000 cm^{-1}) recorded by FTIR spectrophotometer (model: Shimadzu 4300).

RESULTS AND DISCUSSION

XRD analysis: Figure 1 shows the XRD patterns of $Zn_{0.9}Mn_{0.1}O$ calcinated at 400-800°C which confirms that the samples are mostly crystallized in wurtzite structure. The diffraction peaks, belonging to this structure, are indexed in Fig. 1a. The characteristic peaks with high intensity indicate the well crystallization process. These mono-phasic samples, calcinated at 400 and 500°C, reveal that Mn solubility in ZnO structure is increased due to the decrease of the particles size (Straumal *et al*., 2009). So, we have been able to prepare the mono-phase ZnO:Mn nanopowder at low calcination temperatures (400 and 500°C), while the other workers have reported the presence of the secondary phases in the samples prepared at the same calcination temperatures (Jayakumar *et al*., 2006). However, the impurity phases were slightly appeared when the calcination temperature increased to 600°C. Figure 1c shows the two other distinguishable phases crystallized in tetragonal and cubic structures, which are marked with T and C in the figure. With increasing the calcination temperature to 700°C, the tetragonal phase is dominated and the cubic structure is nearly eliminated. In Fig. 1d, the impurity peaks belonging to $Zn(Mn_2)O_4$ with tetragonal symmetry and space group I4/amd are indexed. However, at the calcination temperature of 800°C, we identified that the percentage of the other secondary phase with the cubic symmetry and space group Fd_3m, which relates to $Zn(Mn)O_3$, has clearly increased. For better understanding, the percent of the secondary phases can be roughly estimated from the ratio of the impurity peaks intensity to the total peaks intensity. Figure 2 shows the bar diagram of the calculated percent of the secondary phases of $Zn_{0.9}Mn_{0.1}O$ samples, calcinated at different temperatures.

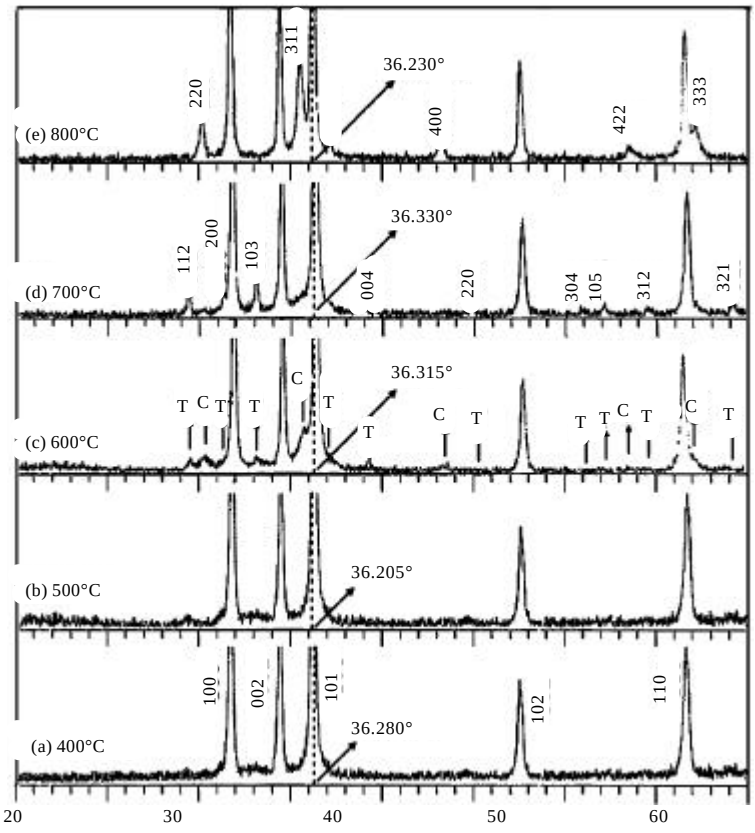

Fig. 1: XRD patterns of $Zn_{0.9}Mn_{0.1}O$ calcinated at different temperatures (a) 400°C, (b) 500°C, (c) 600°C, (d) 700°C and (e) 800°C. The indices in (a), (d) and (e) indicate the peak positions for the wurtzite, tetragonal and cubic structures of ZnO:Mn, respectively

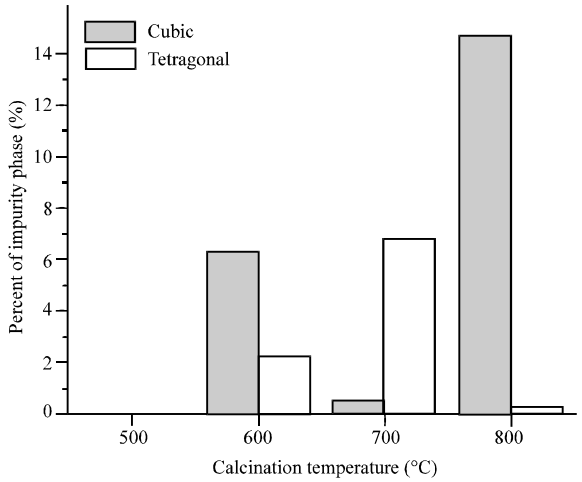

Fig. 2: Bar diagrams present an approximation on each of secondary phases' percentage in $Zn_{0.9}Mn_{0.1}O$ samples calcinated at 500-800°C

As the calcination temperature increases from 600 to 700°C, the percent of the cubic symmetry phase reduces and the tetragonal phase is increased, while at the calcination temperature of 800°C the percentage of these structures in the composition is inversed. The structural properties of the secondary phases are presented in Table 2.

The XRD patterns show that the wurtzite structure is oriented preferably in [101] direction. The intensity ratio of [101] orientation, i_{101}, to the total intensity of other three main peaks has been determined, using the following formula:

$$i_{[101]} = \frac{I_{[101]}}{I_{[100]} + I_{[002]} + I_{[101]}} \times 100 \quad (1)$$

where, I is the peaks intensity obtained from XRD. The calculated values for i_{101}, which are listed in table 1, clarify that the calcination process does not affect the [101] orientation ratio of the wurtzite structure. In addition, the guidelines in Fig. 1 illustrate the changes of [101] peak position of the nanopowders. As shown in this figure, when the calcination temperature changes from 400 to 500°C, the peaks shift to lower angles. On the contrary, the strongest shift towards higher angles has been observed in the sample calcinated at 700°C. These shifts depend directly on the changes of the lattice constants, as discussed by Karamat *et al.* (2008). In the case of decreasing the lattice constants, the peaks shift to higher angles. Thus, we can conclude that decreasing the lattice constants of the sample, calcinated at 700°C, causes the [101] peak shift towards higher angles.

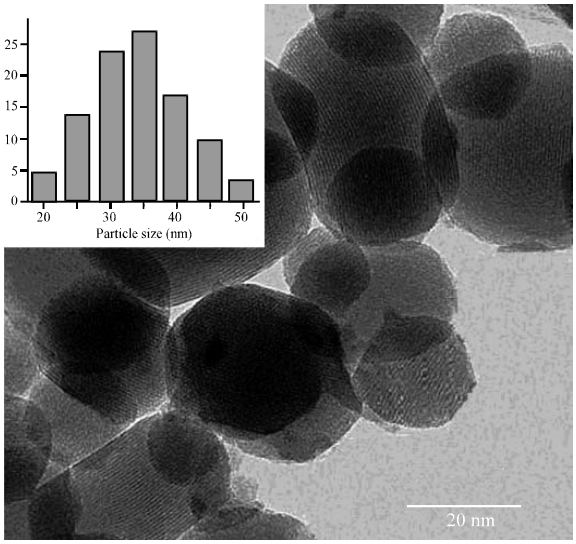

Fig. 3: TEM image of $Zn_{0.9}Mn_{0.1}O$ nanopowder calcinated at 400°C. The inset presents its particle size distribution

Table 1: The variations in [101] orientation percent and lattice parameters due to change of calcination temperature

Calcination temperature (°C)	$i_{[101]}$	$2\theta_{[101]}$	Lattice const. a (Å)	Lattice const. c (Å)
400	46.99	36.280	3.2488	5.2024
500	47.62	36.205	3.2534	5.2127
600	46.66	36.315	3.2465	5.1929
700	47.49	36.330	3.2491	5.1943
800	45.97	36.230	3.2514	5.2081

Table 2: The structural properties of the secondary phases

Calcination temperature (°C)	$2\theta_{[31]}$	Lattice const. a (Å)		Phase (%)
Cubic				
600	35.76	8.369		6.25
800	35.50	8.381		14.7
		Lattice Const.		
Calcination temperature(°C)	$2\theta_{[103]}$	a (Å)	c (Å)	Phase (%)
Tetragonal				
600	33.15	5.716	9.206	2.25
700	33.19	5.714	9.203	6.8

The measured values for the lattice constants, summarized in Table 1, confirm this relation. Increasing the lattice constants is due to the substitution of Mn^{2+} in Zn^{2+} sites, while the decrease of the lattice constants may be related to small portions of Mn^{3+} and Mn^{4+} substitutions in Zn^{2+} sites, instead of Mn^{2+}. The ionic radius of Mn^{3+} (0.58 Å) and Mn^{4+} (0.53 Å) are smaller than the Zn^{2+} (0.60 Å). The ionic radius of Mn^{2+} is 0.66 Å (Bhatti *et al.*, 2005). The IR reflectance spectra support this procedure of ions substitutions, obtained by XRD analysis.

In addition, XRD spectra indicated that Full Width at Half Maximum (FWHM) of [101] peak is approximately constant, in spite of the increase of the calcination

temperature. Thus, it can be deduced that the average particle size must be nearly constant, which is confirmed by Scherrer's relation. The crystalline size of nanopowders, calculated using this relation, was 34.6 nm for the sample calcinated at 400°C which is very close to the value obtained using TEM technique. The TEM image of nanopowders, calcinated at 400°C, is shown in Fig. 3 and the histogram of the particle size distribution is presented in the inset of this figure. The particles have nearly spherical shapes and the average size is estimated to be about 35 nm in diameters.

FTIR analysis: The FTIR transmittance spectra of $Zn_{0.9}Mn_{0.1}O$, with different calcination temperatures, are given in Fig. 4a. The Zn-O stretching mode is clearly observed in all samples, approximately centered at 480 cm^{-1}. This value which shows a shift to higher wavenumbers, in comparison with the bulk ZnO samples (Emelie *et al*., 2006), may depend on the decrease of the particle size to nano scales. However, small deviations from 480 cm^{-1} are observed in the samples having secondary phases. This is due to changes in Zn-O bond properties in tetragonal and cubic structures. Sometimes, FTIR spectrum of ZnO nanopowder presents a shoulder around 510 cm^{-1} as discussed by Kwon *et al*. (2002). We have reported elsewhere (Abrishami *et al*., 2010) that this shoulder sharpened and shifted to higher wavenumbers (620-630 cm^{-1}), due to various contents of Mn as dopant.

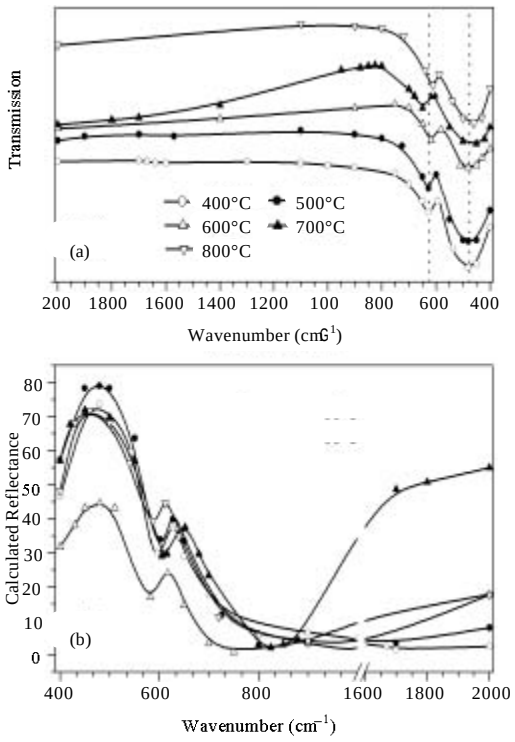

Fig. 4: (a) Transmission and (b) calculated reflectance spectra in Mid-IR Region (400-2000 cm^{-1})

As shown in Fig. 4a, this value for $Zn_{0.9}Mn_{0.1}O$, calcinated at 400 and 500°C, is exactly determined at 625 cm^{-1}. But, this absorption band slightly shifts to 650 cm^{-1} for the sample calcinated at 700°C, which has 14.7% tetragonal phase in the structure. On the contrary, when the percentage of the cubic structure increases, the band moves from 625 to 615 cm^{-1}. In this figure, the guidelines at 480 and 625 cm^{-1} help us to compare the absorption bands.

The calculated reflectance spectra of $Zn_{0.9}Mn_{0.1}O$ calcinated at 400-800°C are given in Fig. 4b. There is a strong band reflection in the range of 400-600 cm^{-1}, called reststrahlen band. Reststrahlen band is dominated by free carrier concentration which did not change effectively by the calcination process, except for $Zn_{0.9}Mn_{0.1}O$ nanopowder prepared at 600°C comprising three different symmetries (wurtzite + tetragonal + cubic). Another important point in the spectra is the high frequencies region dominated by valance electron concentration. Also, Fig. 4b clarifies that the reflection spectrum of $Zn_{0.9}Mn_{0.1}O$, calcinated at 700°C, shows a vigorous increase in this region which is logically concluded as adding extra electrons to the system. This result confirms the XRD analysis about small portion of Mn^{3+} and Mn^{4+} substitutions with Zn^{2+}.

CONCLUSION

$Zn_{0.9}Mn_{0.1}O$ nanopowders were synthesized having interesting advantages such as nano size particles, homogeneity, mono-phasic structure at low calcination temperatures, high Mn solubility and controllable secondary phase percent. In addition, the effect of the calcination process on mid-IR optical properties helped us to express a complete discussion on the phase investigation of ZnO:Mn structures, which confirms the structural properties revealed by XRD analysis.

REFERENCES

Abrishami, M.E., S.M. Hosseini, E.A. Kakhki, A. Kompany and M. Ghasemifard, 2010. Synthesis and structure of pure and Mn-doped zinc oxide nanopowders. Int. J. Nanosci., 9: 19-28.

Bhatti, K.P., S. Chaudhary, D.K. Pandya and S.C. Kashyap, 2005. On the room-temperature ferromagnetism in (ZnO)0.98(MnO2)M0.02.. Solid State Commun., 136: 384-388.

Emelie, P.Y., J.D. Phillips, B. Buller and U.D. Venkateswaran, 2006. Free carrier absorption and lattice vibrational modes in bulk ZnO. J. Elect. Mater., 35: 525-529.

Fonoberov, V.A. and A.A. Balandin, 2006. ZnO quantum dots: Physical properties and optoelectronic applications. J. Nanoelect. Optoelect., 1: 19-38.

Jayakumar, O.D., H.G. Salunke, R.M. Kadam, M. Mohapotra, G. Yaswant and S.K. Kulshreshtha, 2006. Magnetism in Mn-doped ZnO nanoparticles prepared by a co-precipitation method. Nanotechnology, 17: 1278-1285.

Karamat, S., S. Mahmood, J.J. Lin, Z.Y. Pan and P. Lee *et al*., 2008. Structural and magnetic properties of (ZnO)1-x(MnO2)x thin films deposited at room temperature. Applied Surf. Sci., 254: 7285-7289.

Kisi, E.H. and M.M. Elcombe, 1989. Parameters for the wurtzite structure of ZnS and ZnO using powder neutron diffraction. Acta Cryst., 45: 1867-1870.

Kwon, Y.J., K.H. Kim, C.S. Lim and K.B. Shim, 2002. Characterization of ZnO nanopowders synthesized by the polymerized complex method via an organochemical route. Adv. Mater., 3: 146-149.

Noori, N.R., R.S. Mamoory, P. Alizadeh and A. Mehdikhani, 2008. Synthesis of ZnO nanopowder by a gel combustion method. J. Ceram. Process. Res., 9: 246-249.

Ohtaki, M., K. Araki and K. Yamamoto, 2009. High thermoelectric performance of dually doped ZnO ceramics. J. Elect. Mater., 38: 1234-1238.

Straumal, B., B. Bartzky, A. Mazilkin, S. Protasova, A. Myatiev and P. Straumal, 2009. Increase of Mn solubility with decreasing grain size in ZnO. J. Europ. Ceram. Soc., 29: 1963-1970.

Xu, Q., S. Zhou and H. Schmidt, 2009. Magnetic properties of ZnO nanopowders. J. Alloys Compound, 487: 665-667.

Yadav, R.S., A.C. Pandey and S.S. Sanjaya, 2009. Optical properties of Europium doped bunches of ZnO Nanowires Synthesized by co-precipitation method. Chalcogenide Lett., 6: 233-239.